RETRACTIONS

Chem. Eur. J., **2010**, *16*

DOI: 10.1002/chem.200902555

The article "Ultrahighly Sensitive Homogeneous Detection of DNA and MicroRNA Using Single Silver Nanoparticles Counting" by Fagong Xu, Chaoqing Dong, Chao Xie, and Jicun Ren, published online on November 24, 2009 in Wiley Online Library (http://www.onlinelibrary.wiley.com/10.1002/chem.2009002555) and in print (*Chem. Eur. J.* **2010**, *16*, 1010–1016), has been retracted (October 22, 2010) by agreement between the authors, the journal Editor-in-Chief Neville Compton, and Wiley-VCH. The retraction has been agreed due to wrong results on DNA and microRNA hybridization detection by using an incorrect data processing method. The authors regret any confusion that may have been created by the paper's publication.

CHEMISTRY
A EUROPEAN JOURNAL

DOI: 10.1002/chem.200902555

Ultrahighly Sensitive Homogeneous Detection of DNA and MicroRNA by Using Single-Silver-Nanoparticle Counting

Fagong Xu, Chaoqing Dong, Chao Xie, and Jicun Ren*[a]

Abstract: DNA and RNA analysis is of high importance for clinical diagnoses, forensic analysis, and basic studies in the biological and biomedical fields. In this paper, we report the ultrahighly sensitive homogeneous detection of DNA and microRNA by using a novel single-silver-nanoparticle counting (SSNPC) technique. The principle of SSNPC is based on the photon-burst counting of single silver nanoparticles (Ag NPs) in a highly focused laser beam (about 0.5 fL detection volume) due to Brownian motion and the strong resonance Rayleigh scattering of single Ag NPs. We first investigated the performance of the SSNPC system and then developed an ultrasensitive homogeneous detection method for DNA and microRNA based on this single-nanoparticle technique. Sandwich nucleic acid hybridization models were utilized in the assays. In the hybridization process, when two Ag-NP–oligonucleotide conjugates were mixed in a sample containing DNA (or microRNA) targets, the binding of the targets caused the Ag NPs to form dimers (or oligomers), which led to a reduction in the photon-burst counts. The SSNPC method was used to measure the change in the photon-burst counts. The relationship between the change of the photon-burst counts and the target concentration showed a good linearity. This method was used for the assay of sequence-specific DNA fragments and microRNAs. The detection limits were at about the 1 fM level, which is 2–5 orders of magnitude more sensitive than current homogeneous methods.

Keywords: DNA · homogeneous assays · nanoparticles · RNA · silver

Introduction

Nucleic acid analysis is of high importance for clinical diagnoses of infectious and genetic diseases and certain cancers, for forensic analysis, and for basic studies in the biological and biomedical fields. Nucleic acid hybridization is a key biotechnique and is widely used in assays of DNA and RNA. However, conventional heterogeneous formats, such as Northern blotting[1–3] and Southern blotting,[4–6] involve gel electrophoresis, nucleic acid transfers, hybridization reactions, and washing cycles, and even the currently used gene chips (microarrays) need complicated oligonucleotide immobilization and long hybridization and washing steps. Therefore, heterogeneous hybridization formats are considered to be labor intensive and time consuming. The homogeneous hybridization format has long attracted great attention because of its fast hybridization rate and simple operation without washing steps. So far, certain methods have been used in homogeneous nucleic acid hybridization assays, including fluorescence resonance energy transfer,[7–11] molecular-beacon techniques,[12] and fluorescence correlation spectroscopy (FCS),[13–15] but the sensitivity of these homogeneous methods is still unsatisfactory.

Recently, the groups of Mirkin and Muller[16–20] proposed an entirely new colorimetric detection strategy for homogeneous DNA hybridization with gold nanoparticles (GNPs) as probes. The detection principle is based on the strong absorption property and redshift in the absorption spectra of GNPs induced by the aggregation of GNP–oligonucleotide conjugates in the hybridization process. The detection limit is, in general, at the nmol L^{-1} level. Recently, resonance Rayleigh scattering[21–24] and dynamic light scattering[25] techniques were used in homogeneous DNA hybridization with GNPs as probes and the sensitivity was significantly enhanced to about the pmol L^{-1} level. More recently, our group reported a single-GNP counting technique in solution. Based on this single-nanoparticle technique, we developed an ultrasensitive and highly selective detection method for homogeneous immunoassays and DNA hybridization assays

[a] Dr. F. Xu, Dr. C. Dong, Dr. C. Xie, Prof. Dr. J. Ren
College of Chemistry & Chemical Engineering
State Key Laboratory of Metal Matrix Composites
Shanghai Jiaotong University
800 Dongchuan Road, Shanghai 200240 (P.R. China)
Fax: (+86) 21-54741297
E-mail: jicunren@sjtu.edu.cn

Supporting information for this article is available on the WWW under http://dx.doi.org/10.1002/chem.200902555.

by using GNPs as probes, and the detection limits were at the pM and fM levels.[26] In fact, the resonance Rayleigh scattering intensity of silver nanoparticles (Ag NPs) is much stronger than that of the same-size GNPs.[27–29] We reasoned that Ag NPs should be much better as probes than GNPs if the sensitivity of resonance Rayleigh scattering techniques is considered. However, Ag NPs are, in general, used as probes in heterogeneous bioassays,[30–32] and few reports are found on Ag NPs in homogeneous bioassays.[33,34]

Herein, we propose an ultrahighly sensitive homogeneous detection method for DNA and microRNA by using a novel single-silver-nanoparticles counting (SSNPC) technique. The principle of SSNPC is based on the photon-burst counting of single Ag NPs in a highly focused laser beam (about 0.5 fL detection volume) due to Brownian motion and the strong resonance Rayleigh scattering of single Ag NPs. We found that the relationship between the photon-burst counts and the concentration of Ag NPs possessed excellent linearity. On the basis of this single-nanoparticle technique, we developed an ultrasensitive and highly selective homogeneous assay for DNA and microRNA by using the sandwich hybridization strategy and Ag NPs as probes. The detection limits were at about the 1 fM level, which is 2–5 orders of magnitude more sensitive than current homogeneous methods.

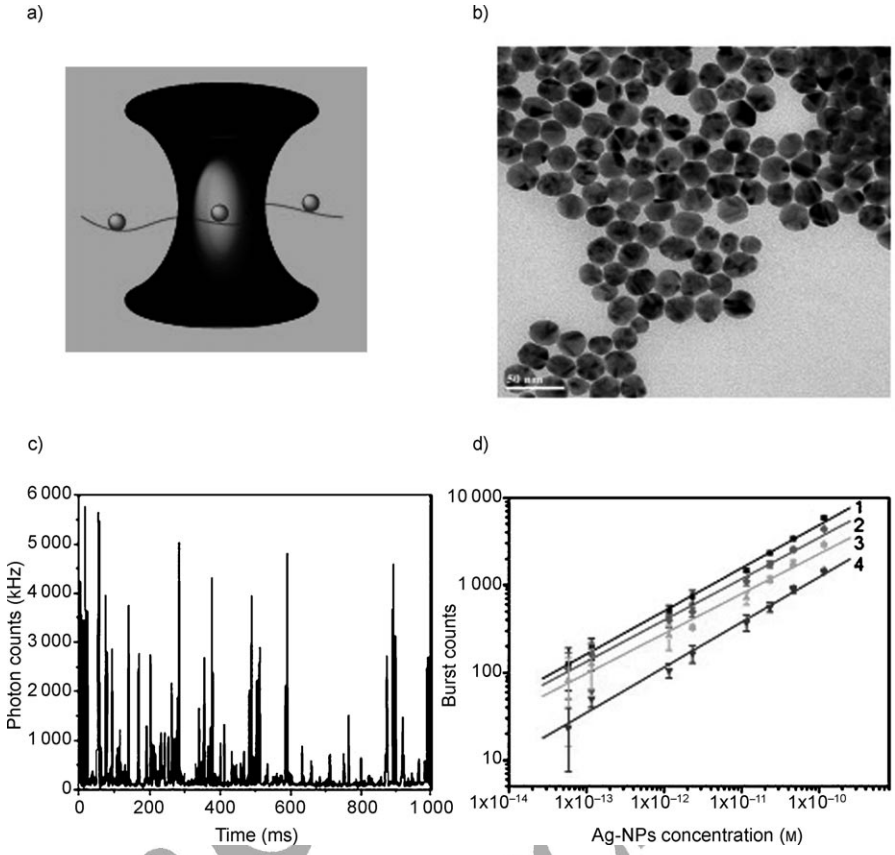

Figure 1. Principle of single-Ag-NP counting and certain experimental results. a) The principle of the single-Ag-NP counting technique. b) TEM images of Ag NPs. The scale bar is 50 nm and the Ag-NP size is about 24 nm. c) Representative photon-bursting trajectory of the Ag-NPs in solution (1.2×10^{-10} M). The benchmark for the time axis was 1 s. d) Relationships between the burst counts and concentration of Ag NPs with different measurement times (lines 1–4: 120, 90, 60, and 30 s, respectively). The linear correlation coefficients are 0.998, 0.996, 0.992, and 0.995, respectively. The linear range (line 1) is 5.8×10^{-14}–1.2×10^{-10} M.

Results and Discussion

SSNPC system: A schematic representation of the SSNPC system is shown in the Supporting Information (Figure S1); the system is similar to the (FCS) system[35] and the single-GNP counting system.[26] Its basic principle is based on the photon-burst counting of single Ag NPs in a highly focused laser beam due to Brownian motion and resonance Rayleigh scattering of single Ag NPs. As shown in Figure 1a, when single Ag NPs diffuse into and out of the small illumination volume through Brownian motion, photon bursting will be generated, which can be monitored in real time by an avalanche photodiode. Figure 1b shows TEM images of Ag NPs used in this study. The average diameter of the Ag NPs is about 24 nm, and the Ag NP sample has a good monodispersity. Figure 1c shows a typical photon-burst trajectory of Ag NPs in solution. We compared the scattering intensity of the 24 nm Ag NPs with the fluorescence intensity of CdTe quantum dots (QDs; emission wavelength of 599 nm) and Rhodamine green (RhG). As shown in Figure 2, the scattering light intensity of single Ag NPs was several tens to hundreds times higher than that of QDs and organic dyes. The strong photon bursting of Ag NPs is mainly attributed to the highly sensitive SSNPC system and the strong resonance scattering of Ag NPs. In the design of the SSNPC system, the key consideration is how to reduce the detection volume to efficiently lower the effects of the background scattering light. In our SSNPC system, the confocal configuration and high numerical aperture objective (NA = 1.2) were used to dramatically reduce the detection volume. We measured the detection volume of SSNPC to be about 0.5 fL by using the FCS method.[35,36] Relative to that of the single-GNP counting system (0.9 fL), the detection volume of SSNPC is significantly decreased. This is because a shorter wavelength (488 nm) laser was used in the SSNPC system, and a longer wavelength (633 nm) laser was used in the single-GNP

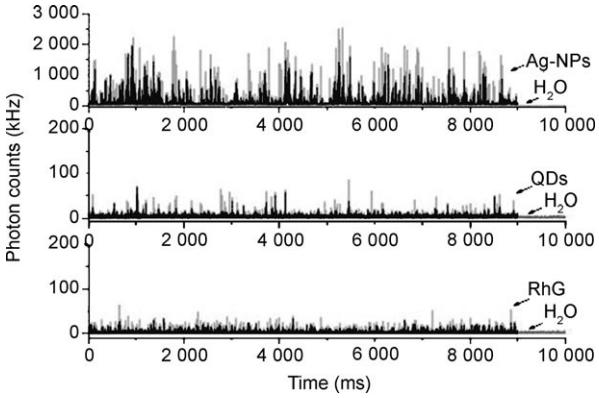

Figure 2. A comparison of the photon-bursting trajectories of Ag NPs (24 nm), quantum dots (CdTe599), and RhG. The Ag-NP concentration was 1.2×10^{-10} M, the QD concentration (emission wavelength of 599 nm) was 5.0×10^{-12} M, and the RhG concentration was 6.8×10^{-11} M. The laser excitation power was 131 μW. The fluorescence of RhG and the QDs was filtered by a band-pass filter (530DF45 and 595AF60, respectively; Omega Optical, USA).

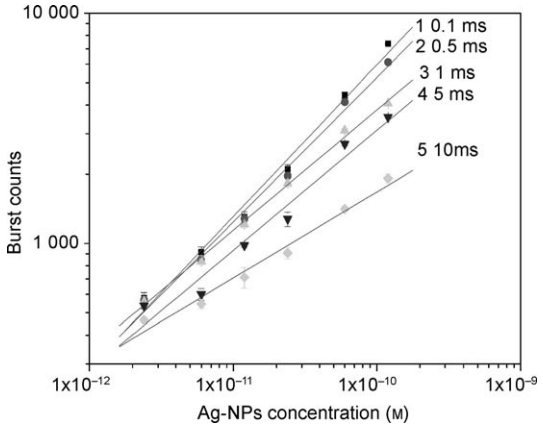

Figure 3. The effects of the bin time on the linear relationship of burst counts and concentration. There are certain differences in the linearity and slope of the curves within our experiment range (0.1, 0.5, 1, 5, and 10 ms). The slopes of the curves are 0.659, 0.628, 0.523, 0.522, and 0.374, respectively. Their correlation coefficients are 0.994, 0.995, 0.998, 0.982, and 0.989, respectively.

counting system. The scattering light intensity of noble-metal nanoparticles (such as GNPs and Ag NPs) is highly dependent on the illumination-light wavelength, so a 488 nm argon laser is suitable for the detection of Ag NPs and a 633 nm He–Ne laser is suitable for the detection of GNPs, in accordance with their resonance scattering spectra. For the confocal configuration, the shorter illumination-light wavelength resulted in the smaller detection volume. In addition, we can use small Ag NPs (24 nm) as probes in this study due to the stronger scattering intensity of Ag NPs. The small Ag NPs were improved the photon-burst counting because of their fast diffusion motion. Figure 1d shows the excellent linear relationship between the photon-burst count and the concentration of Ag NPs. The linear range was from 5.8×10^{-14} to 1.2×10^{-10} M (line 1, $R=0.998$) and the detection limit was 58 fM for 24 nm Ag NPs. Furthermore, we observed that the photon-burst counts of Ag NPs linearly increase with the measurement time (as shown in Figure S2 in the Supporting Information). Interestingly, as shown in Figure 1d, we observed no distinguishable difference in the linearity and slope of the calibration curves within the measurement time range of 30 to 120 s. However, the relative standard deviations (RSDs) of burst counting decreased considerably with the increase in measurement time. We also investigated the effect of the bin time (or time interval) on the photon-burst counts of Ag NPs, and the results are shown in Figure 3. The results showed that the slopes of the curves slightly decreased as the bin time increased within our study range.

We tested the reproducibility of the SSNPC system. The RSDs of the burst counting for intraday and interday were less than 3% ($n=5$) and about 2% ($n=6$), respectively (Figure S3 in the Supporting Information), if the bin time was 1 ms and the measurement time was 120 s. These results demonstrate that the SSNPC method has ultrahigh sensitivity, high spatial resolution (0.5 fL), and good reproducibility.

DNA assays: The principle of the DNA and microRNA assays is shown in Figure 4a and resembles the previously reported sandwich hybridization strategy.[17,21,37] In this study, the target DNA is a 30-base fragment of human p53 gene (exon 8) including a point mutation of C to T.[38–40] The target sequence and its probe sequences are shown in the Experimental Section. We linked two thiol-capped oligonucleotides to Ag NPs through an Ag–S bond. The protocols for linkage of Ag NPs with oligonucleotides are described in the Experimental Section. In the DNA hybridization process, if two Ag-NP–oligonucleotide conjugates are mixed in a sample containing the DNA target, the binding of targets will cause the Ag NPs to form dimers (or oligomers). The number of Ag NPs decreased with an increase in the concentration of targets in the solution, which led to a reduction in the photon-burst counts. The SSNPC system was used to measure the change in the photon-burst counts. Figure 4b and c reflect the photon bursting of Ag-NP–oligonucleotide conjugates in the absence and presence of DNA target. The change in the photon-burst counts of the Ag NPs was mainly attributable to a decrease in the particle number and the diffusion coefficient, due to the formation of larger particles such as dimers in the hybridization reaction. The quantitative detection of the DNA target was based on the dependence of the burst counts on the concentration of DNA target.

Figure 5a illustrates the good linear relationships between the burst counts and the concentration of perfectly complementary target with different final concentrations of Ag-NP–oligonucleotides. The linear ranges were about two orders of magnitude, and the detection limits were 2, 1, and 4 fM for perfectly complementary target DNA, respectively; these values are 2–5 orders of magnitude more sensitive than current homogeneous methods.[34,41–43] In theory, the low initial concentration of nanoparticles improves the sensitivity if the binding constants are high enough. However,

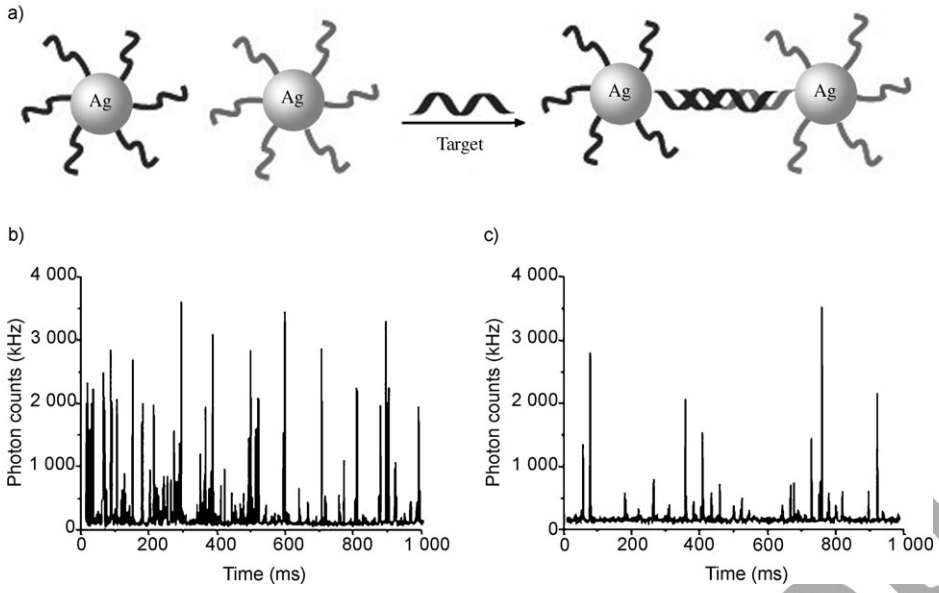

Figure 4. Principle of homogeneous DNA (RNA) hybridization detection. a) Schematic diagram of DNA hybridization. b) Representative photon-bursting trajectory of the Ag-NP–oligonucleotide-conjugate solution before hybridization. c) Representative photon-bursting trajectory of the Ag-NP–oligonucleotide-conjugate solution after hybridization with target DNA.

we observed that the Ag-NP–oligonucleotide concentrations had no significant effect on the assay sensitivity in the study concentration range, as shown in Figure 5a. This is probably due to the low concentration ranges of Ag NPs used in this study.

The specificity of the assay was evaluated by monitoring and analyzing the burst counts arising from a complementary target and mismatched DNA fragments. Figure 5b shows a distribution graph of the burst-count change with the completely complementary DNA fragment (C/G), three single-base-mismatch DNA fragments (C/C, C/T, and C/A), a three-base-mismatch strand (TM), and a noncomplementary strand (NC) as targets in the hybridization. It is obvious that the change of burst counts with the completely complementary strand was very different from that with single-base-mismatch DNA fragments. Furthermore, we observed that, even when the concentration of single-base-mismatch strand (C/A, 200 fM) was 20 times higher than the completely complementary target (10 fM), the photon-burst counts exhibited a significant difference (data shown in Figure 6). In addition, we observed that the hybridization products remained constant for at least 220 min after hybridization (data shown in Figure S4 in the Supporting Information). We tested the reproducibility of this assay and the RSDs were less than 4% (data shown in Figure S5 in the Supporting Information).

MicroRNA assays: Another key application of SSNPC is in the assay of microRNA. MicroRNAs are endogenous noncoding RNAs containing 19–25 nucleotides, and they play important regulatory roles in animals and plants by pairing to the messenger RNA (mRNA) of target genes and specifying mRNA cleavage or repression of protein synthesis.[44] However, microRNAs are short-chain nucleotides, and the assay of these small molecules is very difficult through conventional techniques. Unlike DNA and mRNAs, microRNAs are not easily amplified, which makes microRNA microarray and quantitative PCR techniques challenging.[45–47]

The procedure for the microRNA assay was similar to that for DNA assay described above. Two Ag-NP–oligonucleotide conjugates were used as hybridization probes, and the

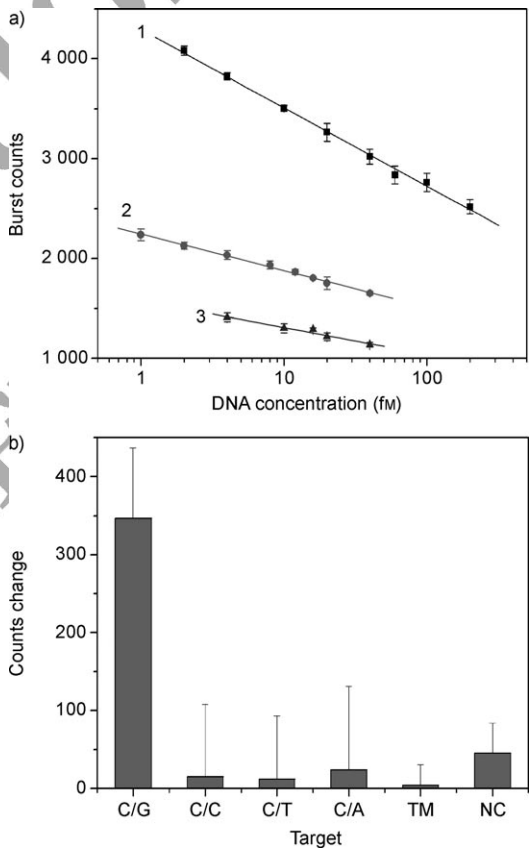

Figure 5. a) Relationships between the burst counts and the perfectly complementary target concentration with different final concentrations (0.1, 0.12, and 0.24 nM) of Ag NPs (24 nm). Line 1: linear range of target: 2–200 fM, $Y=4296–785\ \lg C_{target}$, $R=0.998$; line 2: linear range of target: 1–40 fM, $Y=2246–367\ \lg C_{target}$, $R=0.998$; line 3: linear range of target: 4–40 fM, $Y=1579–269\ \lg C_{target}$, $R=0.982$. b) Distribution graphs of burst-count change from Ag-NP–oligonucleotide conjugates with the complete match DNA fragment (C/G), three single-base-mismatch DNA fragments (C/C, C/T, and C/A), three-base-mismatched strand (TM), and noncomplementary strand (NC) as targets in hybridization. The targets were all at 10 fM concentrations, and the measurement time was 120 s.

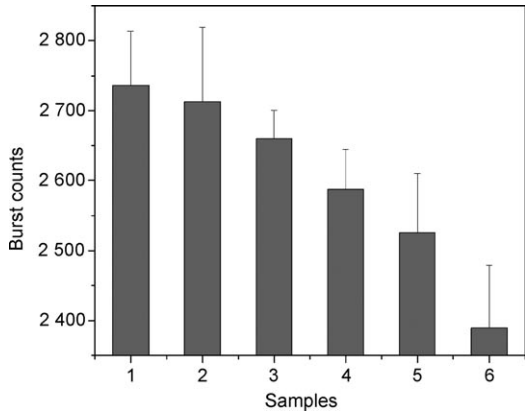

Figure 6. Distribution graphs of burst counts in the absence of target DNA (sample 1) and in the presence of different concentrations of a single-base-mismatched strand (C/A; samples 2–5: 10, 20, 100, and 200 fM, respectively), and 10 fM perfectly complementary target (sample 6). The bin time was 1 ms, and measurement time was 120 s. The error bars represent the standard deviation of five measurements.

SSNPC technique was used to detect the change in the number of Ag NPs in the hybridization solution. Three microRNA sequences and probe sequences are shown in the Experimental Section. Figure 7 shows the good linear rela-

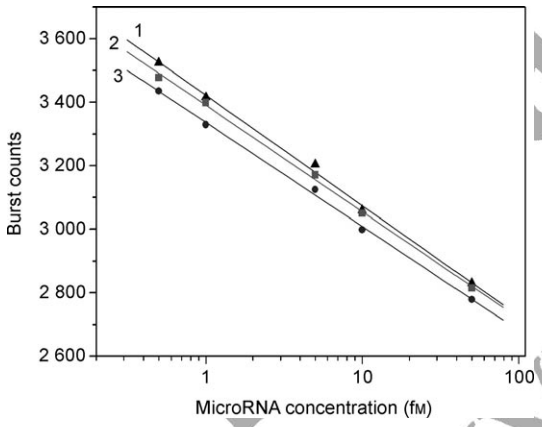

Figure 7. Relationship between the burst counts and the concentrations of microRNAs with 0.24 nM Ag NPs (24 nm). Line 1: linear range of target R21: 0.5–50 fM, $Y=3422–347\ \lg C_{target}$, $R=0.998$; line 2: linear range of target Rp: 0.5–50 fM, $Y=3390–335\ \lg C_{target}$, $R=0.999$; line 3: linear range of target R23a: 0.5–50 fM, $Y=3336–327\ \lg C_{target}$, $R=0.999$. The laser intensity was 131 μW.

tionships between the burst counts and the completely complementary microRNA concentrations. Interestingly, the three calibration curves have similar slopes although their sequences are different. The detection limit for the three microRNAs is about 0.5 fM. Such high sensitivity is due to the use of the SSNPC technique and the DNA-modified Ag-NP probes. It has been reported that GNP probes heavily modified with DNA exhibit a high target-binding constant, which increases the assay sensitivity.[18,48]

In addition, we also observed that the microRNA hybridization products were stable in solution, and the photon-burst counts of the Ag NPs remained constant for at least 195 min after hybridization (data shown in Figure S6 in the Supporting Information). We tested the reproducibility of this assay, and the RSDs were less than 4% (data shown in Figure S7 in the Supporting Information). Our preliminary results document the fact that the SSNPC technique is an ultrasensitive method for characterizing the microRNA level.

Conclusions

In this work, we proposed a novel single-Ag-NP detection method in solution based on the photon bursting of single Ag NPs in a highly focused laser beam due to Brownian motion and resonance scattering. This single-nanoparticle technique was successfully used for one-step homogeneous assays of DNA and microRNAs. The detection limits were about 1 fM, which corresponds to about 1 copy of DNA or microRNA per nL; this value is 2–5 orders of magnitude more sensitive than current homogeneous methods. Importantly, the detection volume of the SSNPC method is about 0.5 fL, and the sample requirement can easily be reduced to the nL level by using the microfluidic droplet technique.[49,50] The assay sensitivity allows the detection of several tens of copies of DNA or RNA when the sample volume is about 10 nL by using droplet arrays. Thus, our method has potential for the direct determination of mRNA and microRNA levels and even genomic DNA in cells, viruses, bacteria, and tissues without PCR and signal amplification.

Experimental Section

Chemicals and instruments: Ag NPs of different size were purchased from Ted Pella, Inc. (USA). All of the DNA oligonucleotides used in this study were purchased from Sangon Biological Engineering Technology & Services Co., Ltd (Shanghai, P.R. China). MicroRNA oligonucleotides used in this study were purchased from TaKaRa Biotechnology Co., Ltd (Dalian, P.R. China).

Ultrapure water with 18.2 $\Omega\,cm^{-2}$ was obtained with a Millipore Simplicity System (Millipore, Bedford, MA, USA). NaH_2PO_4, Na_2HPO_4, and NaCl (Sinopharm Chemical Reagent Co., Ltd, Shanghai, P.R.China) were of analytical reagent grade. All other reagents were used without further purification.

The sequences of DNA[21] and microRNA[47,51] fragments and probes used in this study are given in Table 1 and Table 2, respectively.

Conjugation of oligonucleotides with Ag NPs: Ag-NP–oligonucleotide conjugates were prepared according to the protocol described by Mirkin and co-workers.[52,53] Alkane thiol capped oligonucleotides were centrifuged at 14000 rpm for 5 min and were then dissolved into 10 mM sodium phosphate buffer (pH 7). The final concentration of oligonucleotides was 100 μM. The Ag NPs (24 nm) were further purified prior to use. In brief, Ag NPs (1.0 mL) were concentrated by centrifugation treatment (Beckman Coulter, USA) 2 times at 5000 rpm for 60 min, and the nanoparticle precipitate was washed with ultrapure water (200 μL) and dissolved in ultrapure water (150 μL) prior to use.

Ag NPs were derivatized with alkane thiol capped oligonucleotides (probe 1 or probe 2; final concentration of 5 μM) by incubating the con-

Table 1. DNA fragments and probes used in this study.[21]

DNA	Sequence
probe 1	5′-HS-$(CH_2)_6$-$(A)_{10}$-TTG TGC CTG TCC TGG-3′
probe 2	5′-GAG AGA CCG GCG CAC-$(A)_{10}$-$(CH_2)_6$-SH-3′
perfectly complementary target	5′-GTG CGC CGG TCT CTC CCA GGA CAG GCA CAA-3′
single-base-mismatched strand 1	5′-GTG CGC CAG TCT CTC CCA GGA CAG GCA CAA-3′
single-base-mismatched strand 2	5′-GTG CGC CCG TCT CTC CCA GGA CAG GCA CAA-3′
single-base-mismatched strand 3	5′-GTG CGC CTG TCT CTC CCA GGA CAG GCA CAA-3′
three-base-mismatched strand	5′-GTG GGC CAG TCT GTC CCA GGA CAG GCA CAA-3′
noncomplementary strand	5′-AGT TGT AAG GGA AGA TGC AAT AGT AAT CAG-3′

Table 2. MicroRNA fragments and probes used in this study.[47,51]

MicroRNA	Sequence
hsa-miR-21	5′-UAG CUU AUC AGA CUG AUG UUG A-3′
probe 3	3′-HS-$(CH_2)_6$-$(A)_{10}$-ATC GAA TAG TC-5′
probe 4	3′-TGA CTA CAA CT-$(A)_{10}$- $(CH_2)_6$-SH-5′
hsa-miR-23a	5′-AUC ACA UUG CCA GGG AUU UCC-3′
probe 5	3′-HS-$(CH_2)_6$-$(A)_{10}$-TAG TGT AAC G-5′
probe 6	3′-GTC CCT AAA GG-(A)10- $(CH_2)_6$-SH-5′
hsa-miR-P	5′-CAU CAU GGU CCA GUG CCA GGG-3′
probe 7	5′-GGA CTA TGA TG-$(A)_{20}$-SH-3′
probe 8	5′-SH-$(A)_{20}$-CCC TGG ACA CT-3′

centrated Ag NPs solution (150 μL) described above with a 100 μM probe solution (10 μL) and 10 mM sodium phosphate buffer (pH 7; 40 μL) for 24 h. 1% Bovine serum albumin (BSA; 40 μL) was then added. Over the course of 5–6 h, 2 M NaCl (5 μL) was added to the reaction mixture. After 12 h, more 2 M NaCl (5 μL) was added. The colloids were allowed to age for 6–8 h, then 2 M NaCl (10 μL) was added, and the mixture was left standing for 6–8 h. Finally, the mixture was salted with 0.3 M NaCl. Unbound oligonucleotides were subsequently removed by centrifugation (5000 rpm, 60 min). After removal of the supernatant, the oily precipitate was washed with 0.30 M phosphate buffered saline (PBS; 0.30 M NaCl, 0.125 mg mL^{-1} BSA, pH 7, 10 mM phosphate buffer solution), recentrifuged, and redispersed in 0.30 M PBS. After being washed 3 times, the colloids were resuspended in 0.30 M PBS. Figure S8 in the Supporting Information shows the normalized UV/Vis spectra of the Ag NPs and Ag-NP–oligonucleotide conjugates. It is obvious that the absorption peak has a spectral redshift of about 4 nm and a slight broadening after modification with oligonucleotides. The results were identical with the previously reported ones.[34]

Hybridization procedures: The as-prepared Ag-NP probe 1 (20 μL) and Ag-NP probe 2 (20 μL), each in 0.3 M PBS, were added into a 200 μL sterilized polypropylene tube and mixed well. To the mixed solution, target DNA standard (10 μL) dissolved in 0.3 M PBS was added, and the solutions were mixed well. DNA hybridization was performed on a Gene Amp PCR system 2400 (Applied Biosystems, USA). The mixtures were first heated at 70 °C for 5 min and then quenched to 50 °C for 5 min. After the mixtures had been cooled to room temperature, the sample solution (20 μL) was placed onto a cover slide and assayed by using our SSNPC method. Each solution was measured 5 times, and the measurement time was 120 s.

UV/Vis absorption spectroscopy: The absorption spectra of the Ag-NP colloids and Ag-NP–oligonucleotide conjugates were recorded on a UV-3501 spectrophotometer (Tianjin Gangdong Sci. & Tech. Development Co. Ltd., P.R. China).

Transmission electron microscopy (TEM): TEM images of the nanoparticles were taken with a JEOL 2010F electron microscope (Japan).

SSNPC system: The setup of the SSNPC system is shown in Figure S1 in the Supporting Information and is based on an inverted Olympus IX 71 microscope (Olympus, Japan). An argon ion laser with 488 nm wavelength (Shanghai Ion Laser Co., P.R. China) was reflected by a dichroic mirror (510DRLP, Omega Optical, USA) and then focused into the sample solution by a water immersion objective (UplanApo, 60×NA1.2, Olympus, Japan). The sample was placed on a coverslip (thickness of 170 μm). The scattering signal was collected after passing the 35 μm pinhole by an avalanche photodiode (SPCM-AQR16, Perkin–Elmer EG&G, Canada). The signals obtained were recorded with a real-time digital collector (Flex02–12D/C, Correlator.com, USA). The recording time per sample was 120 s and the bin time was 1 ms.

Data processing and analysis: The photon-burst trajectories of each sample were recorded in real time by the data collector. The data files for each measurement were exported as hexadecimal ASCII files. The decimalized files could be calculated and plotted with the Excel (Microsoft, WA, USA) or Origin (OriginLab Corp., MA, USA) software. Scattering light signals were integrated in 1 ms intervals for a total measurement time of 120 s for each experiment. The photon-burst counts could be obtained by the "pick peaks" tool in the Origin software by using a three-times ratio of signal to noise.

Acknowledgements

This work was financially supported by the NSFC (grant nos.: 20675052, 20727005, and 20975067) and the National Basic Research Program of China (2009CB930400).

[1] O. Franz, I. Bruchhaus, T. Roeder, *Nucleic Acids Res.* **1999**, *27*, 3e.
[2] S. K. Goda, N. P. Minton, *Nucleic Acids Res.* **1995**, *23*, 3357.
[3] E. Várallyay, J. Burgyan, Z. Havelda, *Nat. Protoc.* **2008**, *3*, 190.
[4] E. Southern, *Nat. Protoc.* **2006**, *1*, 518.
[5] Y. L. Sun, Y. Z. Xu, P. Chambon, *Nucleic Acids Res.* **1982**, *10*, 5753.
[6] A. Sunters, K. A. Grimaldi, R. L. Souhami, J. A. Hartley, *Nucleic Acids Res.* **1996**, *24*, 2456.
[7] W. R. Algar, U. J. Krull, *Anal. Chem.* **2009**, *81*, 4113.
[8] R. A. Cardullo, S. Agrawal, C. Flores, P. C. Zamecnik, D. E. Wolf, *Proc. Natl. Acad. Sci. USA* **1988**, *85*, 8790.
[9] M. Masuko, S. Ohuchi, K. Sode, H. Ohtani, A. Shimadzu, *Nucleic Acids Res.* **2000**, *28*, 34e.
[10] S. Sixou, F. C. Szoka, Jr., G. A. Green, B. Giusti, G. Zon, D. J. Chin, *Nucleic Acids Res.* **1994**, *22*, 662.
[11] K. H. Yea, S. Lee, J. Choo, C. H. Oh, *Chem. Commun.* **2006**, 1509.
[12] G. Yao, X. Fang, H. Yokota, T. Yanagida, W. Tan, *Chem. Eur. J.* **2003**, *9*, 5686.
[13] X. Chen, Y. Zhou, P. Qu, X. S. Zhao, *J. Am. Chem. Soc.* **2008**, *130*, 16947.
[14] M. Kinjo, R. Rigler, *Nucleic Acids Res.* **1995**, *23*, 1795.
[15] J. C. Politz, E. S. Browne, D. E. Wolf, T. Pederson, *Proc. Natl. Acad. Sci. USA* **1998**, *95*, 6043.
[16] R. Elghanian, J. J. Storhoff, R. C. Mucic, R. L. Letsinger, C. A. Mirkin, *Science* **1997**, *277*, 1078.
[17] X. Xu, D. G. Georganopoulou, H. D. Hill, C. A. Mirkin, *Anal. Chem.* **2007**, *79*, 6650.
[18] J. J. Storhoff, A. D. Lucas, V. Garimella, Y. P. Bao, U. R. Muller, *Nat. Biotechnol.* **2004**, *22*, 883.
[19] R. A. Reynolds III, C. A. Mirkin, R. L. Letsinger, *J. Am. Chem. Soc.* **2000**, *122*, 3795.
[20] M. S. Han, A. K. R. Lytton-Jean, B. K. Oh, J. Heo, C. A. Mirkin, *Angew. Chem.* **2006**, *118*, 1839; *Angew. Chem. Int. Ed.* **2006**, *45*, 1807.
[21] B. A. Du, Z. P. Li, C. H. Liu, *Angew. Chem.* **2006**, *118*, 8190; *Angew. Chem. Int. Ed.* **2006**, *45*, 8022.

[22] P. C. Ray, *Angew. Chem.* **2006**, *118*, 1169; *Angew. Chem. Int. Ed.* **2006**, *45*, 1151.
[23] K. Wang, X. Qiu, C. Dong, J. Ren, *ChemBioChem* **2007**, *8*, 1126.
[24] X. Liu, Q. Dai, L. Austin, J. Coutts, G. Knowles, J. Zou, H. Chen, Q. Huo, *J. Am. Chem. Soc.* **2008**, *130*, 2780.
[25] Q. Dai, X. Liu, J. Coutts, L. Austin, Q. Huo, *J. Am. Chem. Soc.* **2008**, *130*, 8138.
[26] C. Xie, F. G. Xu, X. Y. Huang, C. Q. Dong, J. C. Ren, *J. Am. Chem. Soc.* **2009**, *131*, 12763.
[27] J. Yguerabide, E. E. Yguerabide, *Anal. Biochem.* **1998**, *262*, 157.
[28] J. Yguerabide, E. E. Yguerabide, *Anal. Biochem.* **1998**, *262*, 137.
[29] J. Yguerabide, E. E. Yguerabide, *J. Cell. Biochem. Suppl.* **2001**, Suppl 37, 71.
[30] I. Tokareva, E. Hutter, *J. Am. Chem. Soc.* **2004**, *126*, 15784.
[31] P. Rijiravanich, M. Somasundrum, W. Surareungchai, *Anal. Chem.* **2008**, *80*, 3904.
[32] C. H. Liu, Z. P. Li, B. A. Du, X. R. Duan, Y. C. Wang, *Anal. Chem.* **2006**, *78*, 3738.
[33] B. C. Vidal Jr., T. C. Deivaraj, J. Yang, H. P. Too, G. M. Chow, L. M. Gan, J. Y. Lee, *New J. Chem.* **2005**, *29*, 812.
[34] D. G. Thompson, A. Enright, K. Faulds, W. E. Smith, D. Graham, *Anal. Chem.* **2008**, *80*, 2805.
[35] C. Dong, H. Qian, N. Fang, J. Ren, *J. Phys. Chem. B* **2006**, *110*, 11069.
[36] S. A. Kim, K. G. Heinze, P. Schwille, *Nat. Methods* **2007**, *4*, 963.
[37] C. Sonnichsen, B. M. Reinhard, J. Liphardt, A. P. Alivisatos, *Nat. Biotechnol.* **2005**, *23*, 741.
[38] E. A. Facher, M. J. Becich, A. Deka, J. C. Law, *Cancer* **1997**, *79*, 2424.
[39] S. N. Rodin, A. S. Rodin, *Proc. Natl. Acad. Sci. USA* **1998**, *95*, 11927.
[40] H. J. vanKranen, A. deLaat, J. vandeVen, P. W. Wester, A. deVries, R. J. W. Berg, C. F. vanKreijl, F. R. deGruijl, *Cancer Res.* **1997**, *57*, 1238.
[41] Y. C. Cao, R. Jin, C. A. Mirkin, *Science* **2002**, *297*, 1536.
[42] R. Jenison, S. Yang, A. Haeberli, B. Polisky, *Nat. Biotechnol.* **2001**, *19*, 62.
[43] G. L. Liu, Y. T. Long, Y. Choi, T. Kang, L. P. Lee, *Nat. Methods* **2007**, *4*, 1015.
[44] W. Wu, M. Sun, G. M. Zou, J. Chen, *Int. J. Cancer* **2007**, *120*, 953.
[45] A. W. Wark, H. J. Lee, R. M. Corn, *Angew. Chem.* **2008**, *120*, 654; *Angew. Chem. Int. Ed.* **2008**, *47*, 644.
[46] L. A. Neely, S. Patel, J. Garver, M. Gallo, M. Hackett, S. McLaughlin, M. Nadel, J. Harris, S. Gullans, J. Rooke, *Nat. Methods* **2006**, *3*, 41.
[47] P. T. Nelson, D. A. Baldwin, L. M. Scearce, J. C. Oberholtzer, J. W. Tobias, Z. Mourelatos, *Nat. Methods* **2004**, *1*, 155.
[48] T. A. Taton, C. A. Mirkin, R. L. Letsinger, *Science* **2000**, *289*, 1757.
[49] W. Shi, J. Qin, N. Ye, B. Lin, *Lab. Chip* **2008**, *8*, 1432.
[50] H. Song, D. L. Chen, R. F. Ismagilov, *Angew. Chem.* **2006**, *118*, 7494; *Angew. Chem. Int. Ed.* 2006, 45, 7336.
[51] S. Griffiths-Jones, *Nucleic Acids Res.* **2004**, *32*, 109D.
[52] J. J. Storhoff, R. Elghanian, R. C. Mucic, C. A. Mirkin, R. L. Letsinger, *J. Am. Chem. Soc.* **1998**, *120*, 1959.
[53] R. Jin, G. Wu, Z. Li, C. A. Mirkin, G. C. Schatz, *J. Am. Chem. Soc.* **2003**, *125*, 1643.

Received: September 16, 2009
Published online: November 24, 2009

